Multidim Syst Sign Process (2018) 29:19–33
https://doi.org/10.1007/s11045-016-0446-8

Applying a modified version of Lyapunov exponent for cancer diagnosis in biomedical images: the case of breast mammograms

Hamed Khodadadi[1] · **Ali Khaki-Sedigh**[2] · **Mohammad Ataei**[3] · **Mohammad Reza Jahed-Motlagh**[4]

Received: 23 August 2015 / Revised: 25 July 2016 / Accepted: 9 August 2016 /
Published online: 26 August 2016
© Springer Science+Business Media New York 2016

Abstract Recently, there has been a great interest in the application of Lyapunov exponents for calculation of chaos levels in dynamical systems. Accordingly, this study aims at presenting two new methods for utilizing Lyapunov exponents to evaluate the spatiotemporal chaos in various images. Further, early detection of cancerous tumors could be obtained by measuring the chaotic indices in biomedical images. Unlike the available systems described by partial differential equations, the proposed method employs a number of interactive dynamic variables for image modeling. Since the Lyapunov exponents cannot be applied to such systems, the image model should be modified. The mean Lyapunov exponent is defined as a chaotic index for measuring the contour borders irregularities in images to detect benign or malignant tumors. Moreover, a two-dimensional mean Lyapunov exponent is incorporated to identify irregularities existing in each axis of the targeted images. Experiments on a set of region of interest in breast mammogram images yielded a sensitivity of 95 % and a specificity of 97.3 % and verified the remarkable precision of the proposed methods in classifying of breast lesions obtained from breast mammogram images.

Keywords Mean Lyapunov exponent · Two-dimensional mean Lyapunov exponent · Partial differential equations · Breast mammograms · Cancer diagnosis · Computer aided diagnosis

✉ Ali Khaki-Sedigh
Sedigh@kntu.ac.ir

1 Department of Electrical and Computer Engineering, Science and Research Branch, Islamic Azad University, Tehran 14778-93855, Iran

2 Department of Electrical Engineering, Industrial Control Center of Excellence, K. N. Toosi University of Technology, Tehran 14317-14191, Iran

3 Department of Electrical Engineering, University of Isfahan, Isfahan 81746-73441, Iran

4 Department of Electrical Engineering, Iran University of Science and Technology, Tehran 16846-13114, Iran

1 Introduction

Images of cancerous tissues have been one of the main motives for developing specific diagnosis tools to detect irregularities in the contour borders of targeted images. Clearly, cancer is usually recognized as a chaotic and poorly regulated growth of cells and tumors. cancerous tumors have irregular forms which cannot be described through common Euclidean geometry (EtehadTavakol et al. 2010). The malignant tumors usually have rough or spiculated blurred boundary contours while benign masses are round, smooth with a well-defined boundary (Rangayyan and Nguyen 2007; Guliato et al. 2008). Consequently, measuring the shape roughness and complexity in contour boundaries could be utilized as two criteria for malignancy and benignity classification based on their related shapes (Rangayyan et al. 2000; Ma and Staunton 2013). In other words, chaos recognition in medical images can lead to early detection of certain cancers (EtehadTavakol et al. 2012).

Similarly, detection of the system behavior by analyzing its image features has been the second motivation of the present study. In some certain systems, the analysis of the image features is the only way for the determination of the system behavior. For instance, some physical systems cannot be described by using specific physical models; and as a result, image may be the only accessible information for their analysis. It is generally known that boundary irregularity associated with targeted images may be due to the chaotic behavior of nonlinear systems. In other words, some irregularities appearing in images are originated from the chaotic behaviors created by the causation processes underlying them. Thus, the distinction between images with irregular and regular boundaries defined by their chaotic and non-chaotic natures requires the application of a new strategy.

Chaotic indices are potentially capable in feature extraction and classification of images. Image processing and compression (Chauveau et al. 2010; Al-Maadeed et al. 2012), image encryption and watermarking (Huang 2011; Shanthi and Bhuvaneswaran 2014), human identity (Yu et al. 2005; Zhao et al. 2008), military applications (Yafei et al. 2007; Zhang 2011) and different medical approaches (EtehadTavakol et al. 2010; Cabral and Rangayyan 2012) are only a few examples representing the mutual relationship between images and chaotic indices. Several indices have been introduced for chaos quantification to study system behavior (Hilborn 2000). The positive Lyapunov exponent (LE) is an index for measuring the hypersensitivity to initial conditions and has been an essential feature of a chaotic system. Thus, the present work aims at utilizing a new approach to extract the mean of Lyapunov exponent (MLE) for images.

As we know, there are few studies on LEs extraction methods for the images. Detecting marine mobile targets (Yang et al. 2008), analyzing the tissues in breast thermal images (EtehadTavakol et al. 2012), feature extracting from hyper-spectral images (Yin et al. 2012), multi-scale analyzing of images (Blasch et al. 2012), detecting pathological carotid artery from ecographic images (Positano et al. 2000) and distinguishing between cancerous cells in Squamous Cell Carcinoma (SCC-61) and normal Mouse Embryonic Fibroblast (MEF) images (Pham and Ichikawa 2013) are some case studies where LEs are calculated on images. The main idea of these studies includes the conversion of image specifications (such as contour boundaries and gray levels of each pixel) into time series, and employing the time series methods of LEs estimation [for instance, reconstructing the phase space using Embedding Dimension (ED) theory].

Clearly, all surveyed studies existing in the literature have the following drawbacks:

– Early studies for LE calculation on the images are based on conversion of images into one dimensional time series. In these studies, image equations and their corresponding features were not examined for chaos detection.
– In some studies, the conversion of a two-dimensional signal, image, into a one-dimensional signal, time series, may lead to losing some features. This means that LE calculation based on the mentioned approaches fails to preserve the image features completely.

To overcome these drawbacks, this paper proposes new approaches using a spatially extended system (SES) model for analyzing the nonlinear indices of the images. Here, parametric deformable model (PDM) which is based on partial differential equation (PDE) is employed for image segmentation. PDE containing interactive variables is used as one of the SES models to detect the spatiotemporal chaos. Since the PDE model of an image contains dynamic variables, some type of modification is performed to provide the necessary condition of LEs estimation.

MLE as the "mean" of LEs is utilized instead of the LE spectrum in the present study. By this new MLE calculation method, it is not necessary to estimate all LEs which is very difficult and time-consuming. Thus, the computational speed rate could be improved. Moreover, employing MLE, the chaos rate and contour boundary irregularities in image can be measured. The concept of two-dimensional mean Lyapunov exponent (2D-MLE) can be also defined via the proposed two-dimensional approach. The new approach is meritorious for several reasons. First of all, it makes possible to detect irregularities along each image axis. Similar to MLE, the speed of calculation may be improved. In addition, adopting 2D-MLE as a diagnostic criterion may lead to higher accuracy classifying.

A variety of simulations on the corresponding region of interest (ROI) in mammogram images are performed to calculate the MLE and 2D-MLE. The ability of the proposed methods in the distinction between the malignant tumors and benign masses is evaluated. Besides, the mammogram images are classified based on their calculated indices. Some classifying performance indices such as sensitivity, specificity and overall accuracy are computed for the classifiers precision assessment. Notably, the LEs estimation hasn't employed as a feature for mammography images in the literature.

The remainder of this paper is organized as follows. Section 2 includes the proposed structure for nonlinear analysis of the images, its modeling based on PDM, MLE and 2D-MLE definitions as well as their calculation. In Sect. 3, MLE and 2D-MLE for a lot of mammogram images are calculated and the normality or abnormality of the mentioned images is distinguished through the proposed methods. Section 4 provides the discussion for the study. Finally, the paper is concluded in Sect. 5.

2 Materials and methods

In this section, the proposed structure for nonlinear analysis of images is presented. In this structure, image is the input of the algorithm while the calculated MLE and 2D-MLE are the outputs. Since the main purpose of the present study is the detection of irregularity in image boundary, the single object image is considered here as the input of the algorithm. More specifically, digitized single contour images with extracted ROI contour boundary are considered as the desired type of input. For other types of single object images, the desired format of input is obtained through the preprocessing stage.

Rescaling the images to a standard size, converting the RGB into a gray-scale, noise removal and converting the resultant image into a binary image are the main steps of pre-

processing stage. Depending on the image type, some of these steps should be utilized. Hence, the only limitation of the method is that the type of images should be in a single object form.

After preprocessing, the image contour boundaries are extracted through the PDM segmentation method. In the next step, the model of image is modified to prepare the model equations for the MLE and 2D-MLE estimation. Finally, in the analysis stage, the MLE and 2D-MLE are calculated on the image. Notably, the obtained MLE and 2D-MLE could be considered as the criteria for classifying different lesions in mammogram images.

2.1 Image modeling based on parametric deformable model

For applying the proposed methods, the primary step is allocating a mathematical model to the image. The internal objects in the images could be extracted using several image segmentation methods. The PDM is a powerful segmentation method based on solving some PDEs. Here, this approach is used to detect the contour boundaries of the image. Analysis of this contour, which is the ROI of the image, could provide valuable information about the image. In the PDM method, a curve is constructed in the image which could be moved by the internal and external forces. The internal forces are designed to keep the model smooth. While, the external forces computed from the image data, are designed to move the model toward an object boundary (Xu et al. 2000; Hsu et al. 2012). The final equation used for the PDM method is given by

$$\gamma \frac{\partial X}{\partial t} = \frac{\partial}{\partial s}\left(\alpha \frac{\partial X}{\partial s}\right) - \frac{\partial^2}{\partial s^2}\left(\beta \frac{\partial^2 X}{\partial s^2}\right) - \nabla P(X), \tag{1}$$

where

$$X(s) = [x(s,t), y(s,t)], \quad s \in [0,1]. \tag{2}$$

Here, γ denotes the damping coefficient introduced to make consistency between the units of the left and right sides, α and β are weighting parameters used for controlling the strength of the model tension and its rigidity and $\nabla P(X)$ describes the energy of the image. Moreover, x and y are the length and width of the image which can be described in terms of contour boundary variable (s) and time (t). Equation (1) couldn't be solved analytically. Thus, a numerical method should be employed to solve it. Considering the discrete variables $X_i^n = \left(x_i^n, y_i^n\right)^T$ in (1) and adopting the finite difference method, yields

$$\begin{aligned}\gamma \frac{X_i^{n+1} - X_i^n}{\Delta t} = & \frac{1}{\Delta h^2}\left[\alpha\left(X_{i+1}^n - 2X_i^n + X_{i-1}^n\right)\right] \\ & - \frac{1}{\Delta h^4}\left[\beta\left(X_{i+2}^n - 4X_{i+1}^n + 6X_i^n - 4X_{i-1}^n + X_{i-2}^n\right)\right] \\ & + F_{ext}(X_i^n), \quad i = 1, \ldots, M, n = 1, \ldots, N,\end{aligned} \tag{3}$$

where i indicates the point number on the contour, n describes the iteration number, Δh and Δt and $F_{ext}(X_i^n)$ are the spatial and time step size and image energy in discrete form, respectively. Equation (3) can be written in a compact form as

$$\begin{aligned}X_i^{n+1} = & X_i^n + \tau \times \frac{1}{\Delta h^2}\left[\alpha\left(X_{i+1}^n - 2X_i^n + X_{i-1}^n\right)\right] \\ & - \tau \times \frac{1}{\Delta h^4}\left[\beta\left(X_{i+2}^n - 4X_{i+1}^n + 6X_i^n - 4X_{i-1}^n + X_{i-2}^n\right)\right] \\ & + \tau \times F_{ext}(X_i^n),\end{aligned} \tag{4}$$

where

$$\tau = \frac{\Delta t}{\gamma}. \tag{5}$$

Equation (4) can be solved using an initial condition (Xu et al. 2000). According to (4), the image could be converted into a PDE with interacting dynamical variables. The PDE is one of the descriptive models of the SES (Schuster and Just 2006) which could represent the spatiotemporal chaos. The obtained equation would be used for calculation of the proposed methods.

2.2 MLE calculation based on the modified equations

The disorderly nature of spatial patterns as a representative of spatiotemporal chaos could be quantified through the MLE calculation (Shibata 1999; Zhao 2003). In this case, the order or disorder of the spatial patterns could be indicated by the small or large values of MLE (Shibata 1999; Behnia et al. 2011). In this section, a new MLE calculation method is presented based on the image equations. This is consistent with the Shibata results presented for MLE estimation of PDEs (Shibata 1999). Consider the following PDE

$$\frac{\partial}{\partial t}\underline{u}(\underline{r}, t) = f(\underline{r}, \underline{u}(\underline{r}, t), t), \tag{6}$$

where $f(\underline{r}, \underline{u}(\underline{r}, t), t)$ denotes a function of the field variable $\underline{u}(\underline{r}, t)$, locus $(\underline{r})$ and time (t). Employing the finite difference method, Eq. (6) becomes

$$\frac{u_j^{k+1} - u_j^k}{\Delta t} = g\left(\Delta x, \left\{u_j^k\right\}\right), \quad j = 1, \ldots, N, k = 1, \ldots, M, \tag{7}$$

where Δt and Δx indicate the time and spatial step size, k and j are the time iteration and discrete locus number, $\left\{u_j^k\right\}$ and g shows a set of field variables and a function of them, respectively. Equation (7) states the relationship between $\left\{u_j^{k+1}\right\}$ and $\left\{u_j^k\right\}$. The Jacobi matrix $(B_{k,N})$ associated with (7) is presented follows

$$B_{k,N} = \begin{pmatrix} \frac{\partial u_1^{k+1}}{\partial u_1^k} & \frac{\partial u_1^{k+1}}{\partial u_2^k} & \cdots & \frac{\partial u_1^{k+1}}{\partial u_N^k} \\ \frac{\partial u_2^{k+1}}{\partial u_1^k} & \frac{\partial u_2^{k+1}}{\partial u_2^k} & \cdots & \frac{\partial u_2^{k+1}}{\partial u_N^k} \\ \vdots & \vdots & \ddots & \vdots \\ \frac{\partial u_N^{k+1}}{\partial u_1^k} & \frac{\partial u_N^{k+1}}{\partial u_2^k} & \cdots & \frac{\partial u_N^{k+1}}{\partial u_N^k} \end{pmatrix}. \tag{8}$$

The Jacobi matrix indicates both the stability of the linear system and its orderly behavior at time k. The MLE introduced by (Shibata 1999) is represented as

$$\lambda_k \equiv \frac{1}{N} \ln \left| B_{k,N} \right|, \tag{9}$$

where $\left| B_{k,N} \right|$ indicates the determinant of matrix $B_{k,N}$. Here, the existence of chaos in (6) is specified with MLE (λ_k). If λ_k gradually increases over time, the chaotic behavior of the spatial pattern of the system could be observed. If the MLE is calculated for different values of the system parameters at the same iteration, the larger exponent value reflects that the system is approaching a chaotic behavior (Shibata 1999).

The MLE defined in (9) can be interpreted as follows: Determinant of the matrix is equal to the product of its eigenvalues. The logarithm converts the multiplication into addition and its averaging will lead to the mean of the logarithm of eigenvalues. This definition completely agrees with the presented concept for the LE in other dynamical systems.

In order to calculate the MLE for the image Eq. (4), The image energy (F_{ext}) should be modified. It is notable that although F_{ext} is completely dependent on position, this dependency doesn't appear explicitly. Therefore, it cannot be used for calculation of the Jacobi matrix. Without considering the image energy, the Jacobi matrix appears the same for all images and cannot distinguish between regular and irregular contour borders. To solve this problem, the cubic interpolation method is employed to approximate the image energy with a third order polynomial function. Another reason for this interpolation is the lack of image energy in all of the desired points and iterations. It is observed that Eq. (4) describes a multi-dimensional interacting system in terms of length and width variables. Through the proposed approximation, the system variables could be separated. This means that Eq. (4) is converted to (10) and (11) for the length and width variables of the image.

$$\begin{aligned} x_i^{n+1} &= x_i^n + \tau \times \frac{1}{\Delta h^2}\left[\alpha\left(x_{i+1}^n - 2x_i^n + x_{i-1}^n\right)\right] \\ &\quad - \tau \times \frac{1}{\Delta h^4}\left[\beta\left(x_{i+2}^n - 4x_{i+1}^n + 6x_i^n - 4x_{i-1}^n + x_{i-2}^n\right)\right] \\ &\quad + \tau \times \left[a_{3xi}^n (x_i^n - x_{i0}^n)^3 + a_{2xi}^n (x_i^n - x_{i0}^n)^2 + a_{1xi}^n (x_i^n - x_{i0}^n) + a_{0xi}^n\right], \end{aligned} \tag{10}$$

$$\begin{aligned} y_i^{n+1} &= y_i^n + \tau \times \frac{1}{\Delta h^2}\left[\alpha\left(y_{i+1}^n - 2y_i^n + y_{i-1}^n\right)\right] \\ &\quad - \tau \times \frac{1}{\Delta h^4}\left[\beta\left(y_{i+2}^n - 4y_{i+1}^n + 6y_i^n - 4y_{i-1}^n + y_{i-2}^n\right)\right] \\ &\quad + \tau \times \left[a_{3yi}^n (y_i^n - y_{i0}^n)^3 + a_{2yi}^n (y_i^n - y_{i0}^n)^2 + a_{1yi}^n (y_i^n - y_{i0}^n) + a_{0yi}^n\right]. \end{aligned} \tag{11}$$

According to (8), the following Jacobi matrix for the (10) and (11) could be obtained.

$$B_{k,2m} = \begin{pmatrix} \frac{\partial x_1^{k+1}}{\partial x_1^k} & \cdots & \frac{\partial x_1^{k+1}}{\partial x_m^k} & \frac{\partial x_1^{k+1}}{\partial y_1^k} & \cdots & \frac{\partial x_1^{k+1}}{\partial y_m^k} \\ \vdots & \ddots & \vdots & \vdots & \ddots & \vdots \\ \frac{\partial x_m^{k+1}}{\partial x_1^k} & \cdots & \frac{\partial x_m^{k+1}}{\partial x_m^k} & \frac{\partial x_m^{k+1}}{\partial y_1^k} & \cdots & \frac{\partial x_m^{k+1}}{\partial y_m^k} \\ \frac{\partial y_1^{k+1}}{\partial x_1^k} & \cdots & \frac{\partial x_m^{k+1}}{\partial y_m^k} & \frac{\partial y_1^{k+1}}{\partial y_1^k} & \cdots & \frac{\partial y_1^{k+1}}{\partial y_m^k} \\ \vdots & \ddots & \vdots & \vdots & \ddots & \vdots \\ \frac{\partial y_m^{k+1}}{\partial x_1^k} & \cdots & \frac{\partial y_m^{k+1}}{\partial x_m^k} & \frac{\partial y_m^{k+1}}{\partial y_1^k} & \cdots & \frac{\partial y_m^{k+1}}{\partial y_m^k} \end{pmatrix}. \tag{12}$$

The rest of calculation is based on Eq. (9). After calculating the determinant of the Jacobi matrix and adopting the required logarithm, the MLE is estimated by averaging of obtained logarithm. As stated previously, the orderly or disorderly behavior of spatial patterns could be quantitatively characterized by the MLE. Therefore, images with irregular contour boundaries have larger values of the MLE compared with regular and smooth ones.

2.3 Developing a two-dimensional mean Lyapunov exponent

Generally, the existing LE computing methods for continuous dynamical system are based on calculating the eigenvalues of the Jacobi matrix. In the eigenvalues of the Jacobi matrix, the gradients of the function are considered and the logarithm of the gradient values indicates the system LEs.

Let to revisit the Jacobi Equation in (12). In this study, the spatial pattern in the image equation consists of two variables; namely, length and width symbolized by x and y. Since it is not possible to solve the equations on a continuous basis, discretization on the length and width of the image are made. Accordingly, the two variables are converted into $2m$ variables; hence, the Jacobi matrix of the system is converted to a matrix with $2m \times 2m$ elements as given in (12). The first mth elements of vector X^n comprise $x_i s$ and the second mth elements include $y_i s$. Therefore, the Jacobi matrix is represented by

$$B_{k,2m} = \begin{pmatrix} B_{xx} & B_{xy} \\ B_{yx} & B_{yy} \end{pmatrix}, \tag{13}$$

where

$$B_{pq} = \begin{pmatrix} \frac{\partial p_1^{k+1}}{\partial q_1^k} & \cdots & \frac{\partial p_1^{k+1}}{\partial q_m^k} \\ \vdots & \ddots & \vdots \\ \frac{\partial p_m^{k+1}}{\partial q_1^k} & \cdots & \frac{\partial p_m^{k+1}}{\partial q_m^k} \end{pmatrix}, \quad p = x, y, \quad q = x, y. \tag{14}$$

Due to the considered cubic interpolation, Eq. (13) could be simplified as

$$B_{k,2m} = \begin{pmatrix} B_{xx} & 0 \\ 0 & B_{yy} \end{pmatrix}. \tag{15}$$

Each submatrix in (13) and (15) is composed of $m \times m$ elements. B_{xx} reflects the effect of $x_j^k s$ on $x_j^{k+1} s$ and the B_{yy} indicates the effect of $y_j^k s$ on $y_j^{k+1} s$ while the other elements are zero. As stated before, the eigenvalues of the Jacobi matrix indicate the gradient values of any function. Thus, by calculating eigenvalues of B_{xx}, the gradient of x_j^{k+1} with respect to x_j^k is computed and its average could be assumed as the mean effect of $x_j^k s$ on $x_i^{k+1} s$.

Note that it is not necessary to estimate all the eigenvalues of a function for computing the mean of them. Since, the trace of a matrix indicates the sum of its eigenvalues, dividing the trace by their number (m) will yield the desired mean. In addition, discretization requirements necessitate us to convert two continuous variables (x and y) of image equations to $2m$ discrete variables. This leads to a redundancy in obtained LEs which could be avoided by the mentioned averaging approach. The Average indicates the effect of each variable at one iteration on other variables at the next iteration. The matrix J_k can be defined as follows

$$J_k = \begin{pmatrix} J_{xx}^k & 0 \\ 0 & J_{yy}^k \end{pmatrix}, \tag{16}$$

where

$$J_{xx}^k = \frac{1}{m} \times trace\left(\frac{\partial x_i^{k+1}}{\partial x_j^k}\right), \quad J_{yy}^k = \frac{1}{m} \times trace\left(\frac{\partial y_i^{k+1}}{\partial y_j^k}\right). \tag{17}$$

The rest of calculation is similar to the continuous systems, where the eigenvalues of matrix J_k is estimated as the (m_i) and then 2D-MLE could be presented as λ_1 and λ_2 through

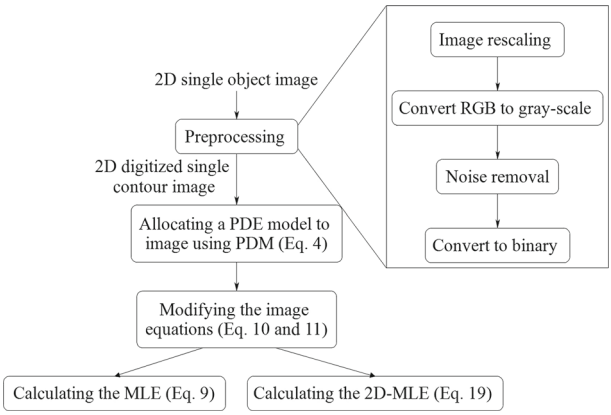

Fig. 1 Flow diagram of the proposed methods

Eq. (19).

$$\det(mI - J_k) = 0, \tag{18}$$

$$\lambda_i = \lim_{t \to 0} \frac{1}{t} \ln |m_i(t)|, \quad i = 1, \ldots, m. \tag{19}$$

According to the diagonal form of (15), λ_1 and λ_2 are the MLEs along the x-axis and the y-axis, respectively. Therefore, 2D-MLE is defined as two exponents in the direction of the x-axis and y-axis. Consequently, the irregularities of the object boundaries of an image along each axis could be detected through the so-defined 2D-MLE. The procedure of the proposed methods for the MLE and 2D-MLE is given in a flowchart shown in Fig. 1.

2.4 Dataset

The suggested methods in this study are implemented for several mammography images. 57 mammogram images are selected in which their normalized ROI relates to the breast masses. This dataset includes 37 ROIs of benign masses and 20 ROIs of malignant tumors (Rangayyan and Nguyen 2007; Cabral and Rangayyan 2012). The normalized ROIs for two benign masses (B1 and B2) as well as two malignant tumors (M1 and M2) of the targeted dataset are presented in Fig. 2. This dataset is employed to evaluate the proposed strategy of several researches such as (Mu et al. 2007; Guliato et al. 2008; Mu et al. 2008).

It should be mentioned that the ROI of breast mammograms is completely different from the original breast mammography images. Generally, detection of the breast masses and extraction of its contour borders is presently an active research area in Computer Aided Diagnosis (CAD) systems of breast mammograms. For instance, automatic contour procedure such as fractal method (Beheshti et al. 2014), maximum likelihood, maximum gradient, hybrid assessment function (Cao et al. 2010), K-means (Oliveira Martins et al. 2009), combination of gradient field information and gray level information (Wei et al. 2005), contour segmentation of breast mass (Berber et al. 2013), improved level set (Liu et al. 2011), semi-automatic contour procedure (Gupta et al. 2011) and manual selection of contour boundaries by expert radiologists (Cabral and Rangayyan 2012) are only some of the approaches considered for the detection of the suspicious mass and extraction of ROI in breast mammograms.

Fig. 2 Contours of the ROIs related to the selected mammogram images, the symbols B and M indicate the benign and malignant cases, respectively (Rangayyan and Nguyen 2007). **a** B1, **b** B2, **c** M1, **d** M2

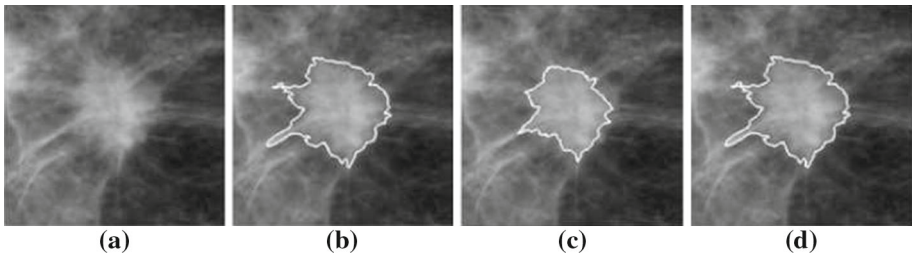

Fig. 3 Segmentation results for one lesion examples. **a** Original image; **b** segmented results based on maximum likelihood analysis; **c** maximum gradient analysis; **d** hybrid assessment function (Cao et al. 2010)

As an example, in Fig. 3 one lesion image of breast mammogram and the segmented results based on three assessment methods proposed by Cao et al. (2010) are illustrated.

It is necessary to mention that the contour of each mass of this dataset images was manually drawn by an expert radiologist specialized in mammography and verified independently by a second radiologist (Rangayyan and Nguyen 2007; Cabral and Rangayyan 2012). In medical images, the contour extraction as a method for boundary detection of objects within an ROI can provide valuable information for diagnosis and treatment of diseases (Hsu et al. 2012). Thus, the contour boundary analysis could be employed to extract the image features. In addition, the ROI of breast mass is completely compatible with the desired input form of this paper as the single object or single contour image.

3 Results

In this section, to investigate the performance of the proposed algorithms in detecting the irregularities in contour boundaries of images, some simulations on the introduced dataset are performed. First step of applying the proposed methods is providing an image description using a mathematical model with modified equations (10, 11). Numerical solution of the mentioned equations converts any initial contour to the main contour. Then, the MLE and 2D-MLE are calculated based on the corresponding equations of the main contour. In all of the simulations, similar number of points are considered in the segmentation stage. Solving (10) and (11) yields the segmented images of B2 and M2 given in Fig. 4.

As could be seen from Fig. 4, the image energy approximation in (10) and (11) has a negligible effect on the segmentation accuracy. In Fig. 4, the segmentation result, the initial and main contours are indicated by solid red, dashed green circle and solid black contour, respectively. In the next step, the corresponding MLEs for all of the study images are

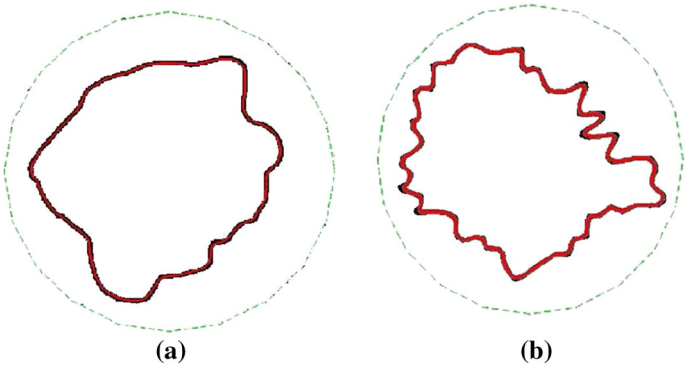

Fig. 4 The segmented images of B2 and M2 based on the modified equations (10) and (11). **a** B2, **b** M2

Table 1 Mean and SD of calculated MLEs and 2D-MLEs for benign and malignant cases

Chaotic indices	MLE		MLE-X		MLE-Y	
Statistical indices	Benign	Malignant	Benign	Malignant	Benign	Malignant
Mean value	−0.2652	−0.1819	−0.1513	−0.1093	−0.1479	−0.1121
SD	±0.0219	±0.0183	±0.0128	±0.0103	±0.0143	±0.0109

calculated and their mean values and standard deviations (SD) for benign and malignant cases are presented in Table 1. According to Table 1, there is a significant difference between the obtained MLEs for benign and malignant cases. Furthermore, the p values are less than 0.05 for both cases indicates the differences are statistically significant. The dataset is classified to demonstrate the effectiveness of the calculated MLE in classifying the normality and abnormality in mammography images. The closeness of obtained MLEs for each of dataset images to the mean values given in Table 1, shows their corresponding category (benign or malignant). Then, true positive (TP) and true negative (TN) as the number of samples which are correctly identified as positives or negatives by the classifier and false negative (FN) and false positive (FP) representing the number of samples corresponding to the cases mistakenly classified as benign or malignant are computed. Afterwards, three evaluation terms; namely, sensitivity, specificity and overall accuracy are computed as 95, 94.6 and 94.7 % respectively. The resulting accuracy indicates that the MLE is an appropriate choice for classifying malignancy and benignity of the targeted tumors. The last step of the simulation involves the calculation of 2D-MLE for the mammogram images of the mentioned dataset. The mean values and SDs of results are illustrated in the same table:

In Table 1, MLE-X is related to the MLE along x-axis, while MLE-Y relates to MLE along y-axis and describe the irregularity of borders for each axis. There is a significant difference between the irregularity of benign and malignant cases for both x and y axes. Hence, it is possible to distinguish between cancerous and normal tissues through calculating either the MLE-X or MLE-Y. In addition, detection of boundary irregularities in the image along its related axis becomes possible through 2D-MLE. For example, the obtained MLE-X for M1 is −0.0961. This value is larger than the MLE-Y of this image (−0.1189) which indicate that the spatial pattern of this image in x-axis is more irregular than its spatial pattern in the y-axis. The p values of 2D-MLE are also less than 0.05 for both cases demonstrating that the results

Table 2 Comparison between accuracy of three classification criteria: LEs based on RPS, MLE and 2D-MLE

Classification performance indices / LEs calculation methods	Sensitivity (%)	Specificity (%)	Accuracy (%)
LEs based on RPS	85	78.4	80.7
MLE	95	94.6	94.7
2D-MLE	95	97.3	96.5

have an acceptable accuracy. Similarly, classification on the dataset is performed through the calculated 2D-MLE. The summation of the differences between the obtained 2D-MLE values for each dataset images and mean values of malignant or benign categories for both MLE-X and MLE-Y is considered as the classification criterion. In this case, evaluation terms such as sensitivity, specificity and overall accuracy for the 2D-MLE are computed which are equal to 95, 97.3 and 96.5 %, respectively. Thus, the introduced 2D-MLE can be considered as an accurate index for differentiating between the normality and abnormality in mammography images.

To compare the performances of the proposed methods with the previous works, the LEs estimation method presented by (EtehadTavakol et al. 2012) is employed to classify the breast mammogram images of the mentioned dataset. Distinction between cancerous and normal tissues by estimating the MLE-X or MLE-Y and the detection of irregularities in borders of images along their axes makes 2D-MLE quite different from the MLE. In addition, the comparison depicted in Table 2 indicates that the 2D-MLE has a higher accuracy than the other LEs calculation methods in terms of contour irregularity measurement and malignancy or benignity classification in breast mammogram images.

4 Discussion

As previously stated, MLE is substituted with LE spectrum in this study. Due to the multiplicity of the variables involved, the estimation of all LEs could be difficult and time-consuming. In addition, since PDEs are utilized to describe the infinite dimensional systems, the estimation of the LE spectrum for such systems will be impossible. Accordingly, the LEs calculation could be lead to computing the largest of them. To solve the problem, the Q-R factorization algorithm (Khaki-Sedigh et al. 2004) and Gram-Schmidt orthogonalization process (Ott 2002) had been utilized. While, in the current method, since the MLE calculation is based on computing the trace or the determinant of Jacobi matrix, it is not necessary to estimate all the LEs. By this approach, the computational complexity is decreased. Therefore, the speed of calculation will be increased. As stated previously, improvement in computational efficiency enhances the performance of some cancer treatment methods which their structures are analyzing the chaotic indices of images.

Another reason for using MLE is non-informative nature of entire LEs of the system under investigation. Although the $2m$ LEs can be obtained from the image segmentation Eqs. (10, 11), the recognition of regular or irregular contour boundaries of the images does not require large numbers of LEs. Similar situations exist in other discrete systems. For example, (Übeyli 2010) calculated 128 LEs for ECG signal. However, the largest LE was selected to detect

heart arrhythmia. The characteristic common to all the mentioned equations is their discrete nature. In continuous systems, the number of LEs is equal to the number of system variables and each of their exponents indicates the system behavior based on its state variables. While in discrete systems, although many variables are produced due to the discretization process, the corresponding eigenvalues contain some redundant information. Thus, a representative exponent, for example, the Largest LE (LLE) or MLE should be selected as a criterion to detect the system behavior. It seems that the MLE is more suitable than LLE due to its higher sensitivity and easier calculation.

Moreover, as previously mentioned, the irregularity in contour borders of images is the result of their chaotic dynamics. It is known that malignant and cancerous tumors have more chaotic dynamics than benign ones. Simulation results demonstrate that malignant tumors with irregular contour boundaries have greater values of MLE than benign masses with regular boundaries. Thus, the proposed indices can be introduced as indicators representing the rate of chaos in images. The high precision results obtained from mammogram images classified by the MLE and 2D-MLE show that they are potentially suitable for image classification.

Clearly, for a dissipative system, the sum of LEs must be negative (Hilborn 2000). This means that the existence of some positive LEs in Lyapunov spectrum of chaotic systems does not lead to a positive MLE. Although the MLE for both the chaotic and deterministic systems (i.e. irregular and regular contour borderlines in this study) is negative, the corresponding values obtained for chaotic systems are higher than the deterministic ones.

Generally, the CADs are procedures in medicine that assist doctors in the interpretation of medical images. With CAD, the computer output is considered as a *second opinion* for radiologists to make the final decision. In other words, CAD is not the substitution of the doctor in medical diagnosis, albeit has a complementary effect (Doi 2007; Fujita et al. 2012; Larvie et al. 2016). Therefore, the obtained results of diagnosis the malignancy or benignity through the proposed methods can offer complimentary computing power to improve the medical examination ability of physicians.

5 Conclusion

Detection of regularity or irregularity of object boundaries in medical images is important for the determination of chaotic behavior of different systems and early detection of cancerous tissues and tumors. Therefore, it is necessary to evaluate the chaotic behavior of images through empirically specified criteria. The present study focuses on the application of a two-dimensional PDE for creating a reliable model of image. The MLE, as the modified version of LE, is utilized to detect the spatiotemporal chaos in the studied images. With the modification of image model equations, the MLE calculation on an image results in the distinguishing between its regular and irregular borderlines. The obtained two-dimensional equation of the image is employed to extend the concept of MLE to 2D-MLE. Consequently, the calculation of 2D-MLE facilitates the detection of irregularities in contour borders of an image existing along its axis. The non-informative nature of the image LE spectrum and resultant computational speed rate improvement encourage us to employ MLE instead of LE spectrum.

Experimental results on a set of breast mammograms containing malignant and benign cases substantiate the credibility of the claims about the distinction between images with regular and irregular borders. The high accuracy of the proposed methods demonstrates their satisfactory efficiency for classifying the malignancy and benignity of the body tissues which is a central factor in the diagnosis of cancerous tumors.

References

Al-Maadeed, S., Al-Ali, A., & Abdalla, T. (2012). A new chaos-based image-encryption and compression algorithm. *Journal of Electrical and Computer Engineering*, *2012*, 1–11.

Beheshti, S., AhmadiNoubari, H., Fatemizadeh, E., & Khalili, M. (2014). An efficient fractal method for detection and diagnosis of breast masses in mammograms. *Journal of Digital Imaging*, *27*(5), 661–669.

Behnia, S., Panahi, M., Akhshani, A., & Mobaraki, A. (2011). Mean Lyapunov exponent approach for the helicoidal Peyrard–Bishop model. *Physics Letters A*, *375*(41), 3574–3578.

Berber, T., Alpkocak, A., Balci, P., & Dicle, O. (2013). Breast mass contour segmentation algorithm in digital mammograms. *Computer Methods and Programs in Biomedicine*, *110*(2), 150–159.

Blasch, E. P., Gao, J., & Tung, W.-W. (2012). Chaos-based image assessment for THz imagery. In *2012 11th International conference on information science, signal processing and their applications (ISSPA)* (pp. 360–365). IEEE.

Cabral, T. M., & Rangayyan, R. M. (2012). Fractal analysis of breast masses in mammograms. *Synthesis Lectures on Biomedical Engineering*, *7*(2), 1–118.

Cao, Y., Hao, X., Zhu, X., & Xia, S. (2010). An adaptive region growing algorithm for breast masses in mammograms. *Frontiers of Electrical and Electronic Engineering in China*, *5*(2), 128–136.

Chauveau, J., Rousseau, D., & Chapeau-Blondeau, F. (2010). Fractal capacity dimension of three-dimensional histogram from color images. *Multidimensional Systems and Signal Processing*, *21*(2), 197–211.

de Oliveira Martins, L., Junior, G. B., Silva, A. C., de Paiva, A. C., & Gattass, M. (2009). Detection of masses in digital mammograms using k-means and support vector machine. *ELCVIA: Electronic Letters on Computer Vision and Image Analysis*, *8*(2), 39–50.

Doi, K. (2007). Computer-aided diagnosis in medical imaging: Historical review, current status and future potential. *Computerized Medical Imaging and Graphics*, *31*(4), 198–211.

EtehadTavakol, M., Lucas, C., Sadri, S., & Ng, E. (2010). Analysis of breast thermography using fractal dimension to establish possible difference between malignant and benign patterns. *Journal of Healthcare Engineering*, *1*(1), 27–44.

EtehadTavakol, M., Ng, E., Lucas, C., Sadri, S., & Ataei, M. (2012). Nonlinear analysis using Lyapunov exponents in breast thermograms to identify abnormal lesions. *Infrared Physics & Technology*, *55*(4), 345–352.

Fujita, H., Nogata, F., Jiang, H., Kido, S., Feng, T., Hara, T., et al. (2012). Medical image processing and computer-aided detection/diagnosis (CAD). In *2012 International conference on computerized healthcare (ICCH)* (pp. 66–71). IEEE.

Guliato, D., de Carvalho, J. D., Rangayyan, R. M., & Santiago, S. A. (2008a). Feature extraction from a signature based on the turning angle function for the classification of breast tumors. *Journal of Digital Imaging*, *21*(2), 129–144.

Guliato, D., Rangayyan, R. M., Carvalho, J. D., & Santiago, S. A. (2008b). Polygonal modeling of contours of breast tumors with the preservation of spicules. *IEEE Transactions on Biomedical Engineering*, *55*(1), 14–20.

Gupta, S., Sadiq, M., Gupta, M., & Rao, N. (2011). Semi-automatic segmentation of breast cancer for mammograms based on watershed segmentation. In *Proceedings of the 5th national conference for nation development*.

Hilborn, R. C. (2000). *Chaos and nonlinear dynamics: An introduction for scientists and engineers*. Oxford: Oxford University Press.

Hsu, R. C., Chan, D. Y., Liu, C.-T., & Lai, W.-C. (2012). Contour extraction in medical images using initial boundary pixel selection and segmental contour following. *Multidimensional Systems and Signal Processing*, *23*(4), 469–498.

Huang, X. (2011). Image encryption algorithm using chaotic Chebyshev generator. *Nonlinear Dynamics*, *67*(4), 2411–2417.

Khaki-Sedigh, A., Ataei, M., Lohmann, B., & Lucas, C. (2004). Adaptive calculation of Lyapunov exponents from time series observations of chaotic time varying dynamical systems. *Nonlinear Dynamics and Systems Theory*, *4*, 145–159.

Larvie, J., Sefidmazgi, M., Homaifar, A., Harrison, S., Karimoddini, A., & Guiseppi-Elie, A. (2016). Stable gene regulatory network modeling from steady-state data. *Bioengineering*, *3*(2), 12.

Liu, J., Chen, J., Liu, X., Chun, L., Tang, J., & Deng, Y. (2011). Mass segmentation using a combined method for cancer detection. *BMC Systems Biology*, *5*(3), 1–9.

Ma, L., & Staunton, R. C. (2013). Analysis of the contour structural irregularity of skin lesions using wavelet decomposition. *Pattern Recognition*, *46*(1), 98–106.

Mu, T., Nandi, A. K., & Rangayyan, R. M. (2007). Classification of breast masses via nonlinear transformation of features based on a kernel matrix. *Medical & Biological Engineering & Computing*, *45*(8), 769–780.

Mu, T., Nandi, A. K., & Rangayyan, R. M. (2008). Classification of breast masses using selected shape, edge-sharpness, and texture features with linear and kernel-based classifiers. *Journal of Digital Imaging*, *21*(2), 153–169.

Ott, E. (2002). *Chaos in dynamical systems*. Cambridge: Cambridge University Press.

Pham, T. D., & Ichikawa, K. (2013). Spatial chaos and complexity in the intracellular space of cancer and normal cells. *Theoretical Biology & Medical Modelling*, *10*, 62.

Positano, V., Mammoliti, R., Benassi, A., Landini, L., & Santarelli, M. (2000). Nonlinear analysis of carotid artery echographic images. *IEE Proceedings-Science, Measurement and Technology*, *147*(6), 327–332.

Rangayyan, R. M., Mudigonda, N. R., & Desautels, J. E. L. (2000). Boundary modelling and shape analysis methods for classification of mammographic masses. *Medical & Biological Engineering & Computing*, *38*(5), 487–496.

Rangayyan, R. M., & Nguyen, T. M. (2007). Fractal analysis of contours of breast masses in mammograms. *Journal of Digital Imaging*, *20*(3), 223–237.

Schuster, H . G., & Just, W. (2006). *Deterministic chaos: An introduction*. London: Wiley.

Shanthi, P., & Bhuvaneswaran, R. (2014). Robust chaos based image watermarking scheme for fractal-wavelet. *Applied Mathematical Sciences*, *8*(32), 1593–1604.

Shibata, H. (1999). Lyapunov exponent of partial differential equation. *Physica A*, *264*(1), 226–233.

Übeyli, E. D. (2010). Recurrent neural networks employing Lyapunov exponents for analysis of ECG signals. *Expert Systems with Applications*, *37*(2), 1192–1199.

Wei, J., Sahiner, B., Hadjiiski, L. M., Chan, H.-P., Petrick, N., Helvie, M. A., et al. (2005). Computer-aided detection of breast masses on full field digital mammograms. *Medical Physics*, *32*(9), 2827–2838.

Xu, C., Pham, D. L., & Prince, J. L. (2000). Image segmentation using deformable models. *Handbook of Medical Imaging*, *2*, 129–174.

Yafei, Z., Minhui, Z., & Jinsong, C. (2007). Distributed target detection in SAR images using improved chaos-based method. In *2007 IEEE international geoscience and remote sensing symposium* (pp. 929–932). IEEE.

Yang, S., He, S., & Lin, H. (2008). Video Image Targets Detection Based on the largest Lyapunov exponent. In *2008 The 9th international conference for young computer scientists* (pp. 2973–2977). IEEE.

Yin, J., Gao, C., & Jia, X. (2012). Using Hurst and Lyapunov exponent for hyperspectral image feature extraction. *IEEE Geoscience and Remote Sensing Letters*, *9*(4), 705–709.

Yu, L., Zhang, D., Wang, K., & Yang, W. (2005). Coarse iris classification using box-counting to estimate fractal dimensions. *Pattern Recognition*, *38*(11), 1791–1798.

Zhang, Y. (2011). Chaotic analysis of ocean clutter. In *2011 4th International congress on image and signal processing* (Vol. 5, pp. 2720–2724). IEEE.

Zhao, L., Ma, N., & Xu, X. (2008). Face recognition based on fractal dimension. In *2008 7th World congress on intelligent control and automation* (pp. 6830–6833). IEEE.

Zhao, Y. (2003). *Introduction to some methods of chaos analysis and control for PDEs. Lecture notes in control and information sciences* (Vol. 292). Berlin: Springer.

Hamed Khodadadi received his B.S. degree in control engineering from Iran University of Science & Technology in 2005, and the M.Sc. in control engineering from Islamic Azad University, Science and Research Branch (SRB) in 2009. Currently, he is a Ph.D. student of control engineering in Islamic Azad University, SRB and a faculty member of Technical and Engineering Department in Islamic Azad University at Khomeinishahr, Isfahan, Iran. His current research interests are control theory, chaotic systems, image processing and Computer Aided Diagnosis (CAD).

Ali Khaki-Sedigh is currently a professor of control systems with the Department of Electrical Engineering, K. N. Toosi University of Technology, Tehran, Iran. He obtained an honors degree in mathematics in 1983, a master's degree in control systems in 1985 and a Ph.D. in control systems in 1988, all in the UK. He is the author and co-author of about 90 journal papers, 170 international conference papers and has published 14 books in the area of control systems. His main research interests are adaptive and robust multivariable control systems, complex systems and chaos control, research ethics and the history of control.

Mohammad Ataei received the B.Sc. degree from the Isfahan University of Technology, Iran, in 1994, the M.Sc. degree from the Iran University of Science & Technology, Iran, in 1997, and Ph.D. degree from K. N. University of Technology, Iran, in 2004 (joint project with the University of Bremen, Germany) all in control Engineering. He is associate professor at the Department of Electrical Eng. at University of Isfahan, Iran. His main areas of research interest are control theory and applications, nonlinear control, and chaotic systems' analysis and control.

Mohammad Reza Jahed-Motlagh received his B.Sc. degree in Electrical Engineering in 1978 from the Sharif University of Technology, Tehran, Iran, and his M.Sc. and Ph.D. degrees in Control Engineering in 1986 and 1990, both from the University of Bradford, Bradford, UK. He is currently an Associate Professor of Iran University of Science and Technology, Tehran, Iran. His research interests include complex systems, nonlinear systems, and artificial intelligence.